ELSEVIER

Journal of Chromatography A, 857 (1999) 69–87

JOURNAL OF CHROMATOGRAPHY A

www.elsevier.com/locate/chroma

Influence of column radial heterogeneity on peak fronting in linear chromatography

Kanji Miyabe[a,b], Georges Guiochon[a,b,*]

[a]*Department of Chemistry, The University of Tennessee, Knoxville, TN 37996-1600, USA*
[b]*Division of Chemical and Analytical Sciences, Oak Ridge National Laboratory, Oak Ridge, TN 37831, USA*

Received 29 December 1998; received in revised form 16 June 1999; accepted 18 June 1999

Abstract

Using numerical calculations of elution peak profiles, an explanation of the fronting behavior of elution peaks in linear chromatography was found in certain radial distributions of the mobile phase flow velocity and local bed efficiency. Fronting peaks are observed only if the flow velocity is higher in the wall region than in the center part of the column and the local efficiency is lower near the wall than in the center. By contrast, tailing or symmetrical peaks are observed if only the flow velocity or the local efficiency are radially heterogeneous. The degree of peak fronting increases with increasing amplitude of the radial distributions. The influence of the radial heterogeneity of the flow velocity on the degree of peak fronting is more severe for high than for low efficiency columns. An equation is suggested to correlate peak fronting behavior for columns of different efficiencies and a procedure proposed for the estimation of the radial distributions of the flow velocity and the local efficiency by analyzing some characteristics of asymmetric peaks.

Keywords: Column radial heterogeneity; Peak shape; Column efficiency; Flow velocity distribution

1. Introduction

In principle, the elution profiles of chromatographic bands are affected by the characteristics of the thermodynamics of equilibrium between the two phases of the system and by the kinetics of mass transfer between them [1]. In preparative chromatography, band profiles should be interpreted first on the basis of the equilibrium thermodynamics which has the stronger influence [1]. By contrast, the role of mass transfer kinetics on peak profiles is the only important one in linear chromatography because a linear equilibrium isotherm provides no influence on the shape of elution peaks. Accordingly, it is often assumed that, as a first approximation, peak profiles in linear chromatography should be well accounted for by a Gaussian distribution function. However, tailing and/or fronting profiles are often observed under experimental conditions corresponding to proven linear isotherms. Peak asymmetry has been for more than fifty years and remains to this day a knotty problem in physico–chemical studies involving chromatography as a topic or a mean of investigation because most equations in linear chroma-

*Corresponding author. Corresponding address: Department of Chemistry, The University of Tennessee, Buehler Hall, Knoxville, TN 37996-1600, USA. Tel.: +1-423-9740-733; fax: +1-423-9742-667.
E-mail address: guiochon@utk.edu (G. Guiochon)

0021-9673/99/$ – see front matter
PII: S0021-9673(99)00752-9

tography are derived from the Gaussian function. Thus, it still is a relevant problem to attempt elucidating the cause of the asymmetry of chromatographic peaks.

Many interpretations and models were proposed to explain unsymmetrical peaks [1,2]. Early conventional studies on peak tailing suggested three causes of instrumental origin, a tailing injection profile, a slow detector response and a significant dead volume in tubing connections. In addition to these extra-column sources, heterogeneous mass transfer kinetics is considered as an essential origin of peak tailing. Guiochon et al. [1] and Fornstedt et al. [3,4] reported the results of detailed studies on the origin of peak tailing in both linear and nonlinear chromatography. They made numerical calculations using a transport–dispersive model and provided a comprehensive interpretation for peak tailing on the basis of a two-site model, in which the presence of two different types of adsorption sites with different equilibrium isotherms and rates of mass transfer kinetics were assumed. The two-site model is especially relevant in the case of chiral separations or in the analysis of strong bases by reversed-phase liquid chromatography (RPLC) because, in these cases, there are strong selective interactions between the sample components and certain sites on the surface of the stationary phase.

Recent investigations have shown that most columns are radially heterogeneous to a degree and that this heterogeneity is another source of peak tailing. Farkas et al. [5,6] and Farkas and Guiochon [7] determined the radial distributions of the mobile phase flow velocity, the local efficiency [i.e., its height equivalent to a theoretical plate (HETP)], and the concentration of a compound for several slurry packed columns by using fiber optics and on-column local fluorescence detection. Yun and Guiochon [8] photographically demonstrated that bands in large diameter columns are radially heterogeneous. These studies confirm previous results obtained in high-performance liquid chromatography (HPLC) [9–14]. They are in excellent agreement with those derived from investigations of the local dispersion in similar columns by pulsed field gradient (PFG)-nuclear magnetic resonance (NMR) methods [15–18]. They supply new information regarding the extent of the column radial heterogeneity.

For example, it was demonstrated that the flow velocity of the mobile phase was several percent lower in the wall region than in the column center while the HETP was several times larger near the wall than in the center region. The radial distributions of the flow velocity and the HETP in the columns studied were accounted for by parabolic functions. The amplitudes of the variations of the velocity and the efficiency across the column were correlated with the apparent efficiency of the column, i.e., the efficiency derived from the elution peak recorded with a detector operating on the bulk eluent. On the basis of these experimental results, Miyabe and Guiochon [19,20] studied the correlation between peak tailing and the extent of the column radial heterogeneity in linear chromatography, using a numerical method to calculate axial band profiles. Finally, Yun and Guiochon [21,22] realized that the systematic investigations of moderately heterogeneous columns, which have a cylindrical symmetry, require the development of tools allowing the integration of the mass balance equation of chromatography in a two-dimensional space. They proposed such a model applicable under nonlinear conditions. The tailing peaks of nonretained tracers or of compounds capable only of hydrophobic interactions with the stationary phase can be explained by considering the radial heterogeneity of the column as well as the peaks of any retained compounds.

As described above, several different interpretations and models are available to account for peak tailing phenomena. By contrast, there are few studies on peak fronting although this behavior is also observed in practice. It is well known that fronting peak are observed in preparative chromatography when the equilibrium isotherm is convex downward, i.e., toward the axis of mobile phase concentrations. However, peak fronting in linear chromatography cannot be explained by either the thermodynamic properties of the phase equilibrium or the mass transfer kinetics. This shows that we need another interpretation. This paper deals with the possible influence on peak fronting of the radial distribution of the mobile phase flow velocity and of the local efficiency. As explained earlier, it is observed that all conventional HPLC columns exhibit a degree of radial heterogeneity [23]. We simply do not know how to pack completely homogeneous columns.

Therefore, it is useful to clarify the possible correlation between the column radial heterogeneity and the direction and nature of the asymmetry of the elution peaks. The characteristic features of various fronting peaks were calculated assuming different models of column radial heterogeneity and they were analyzed. Conversely, the comparison of the calculation results with some experimental data provided new information on the column radial heterogeneity.

2. Theory

We calculated elution peak profiles, using the numerical solution of the equilibrium–dispersive model, on the basis of the following assumptions.

1. The equilibrium isotherm is linear.
2. The column is hypothetically divided into coaxial 50 annular columns having a constant thickness, equal to 1/50 radius of the column.
3. Each of these annular columns is considered as homogeneous, hence and the profile of a peak eluting from each of these annular column would be Gaussian.
4. The radial distributions of the mobile phase flow velocity and of the local value of the dispersion coefficient are represented by parabolic functions.
5. There is no radial dispersion of a sample substance in the column.
6. The overall elution peak from the radially heterogeneous column is obtained as the sum of each individual Gaussian profile weighed in proportion to the cross-section area of the corresponding annular column.

The following equations and correlations were used for the numerical calculation of each of the elution peaks [1]. The Gaussian profile of the elution peak from each annular column is given by

$$C_d = \frac{1}{\sigma_d\sqrt{2\pi}} \exp\left(-\frac{(1-t_d)^2}{2\sigma_d^2}\right) \quad (1)$$

where C_d, t_d and σ_d are the dimensionless concentration, time and standard deviation of the Gaussian peak, respectively. The first two parameters are derived as follows.

$$C_d = \frac{Ct_R}{A_p} = \frac{C\epsilon SL(1+k_0')}{n} \quad (2)$$

$$t_d = \frac{t}{t_R} = \frac{ut}{L(1+k_0')} \quad (3)$$

where C is the actual solute concentration, t_R its retention time, A_p the area of the injected pulse, ϵ the total porosity of the column, S and L the column cross-sectional area and length, respectively, k_0' the retention factor at infinite dilution, n the amount of the solute injected, t the time, and u the interstitial velocity of the mobile phase.

The radial distribution of the mobile phase flow velocity and the apparent axial dispersion coefficient are represented by parabolic functions, in agreement with the results of Farkas and co-workers [5–7] and Baur et al. [13,14] who demonstrated distributions of this type in slurry-packed columns. Knox et al. [11] and Eon [12] also showed similar results for dry packed glass beads columns although the curvature of the distribution of the mobile phase flow velocity was opposite, higher near the wall than in the core region of the column

$$u_r = a_u\left(\frac{r}{R}\right)^2 + b_u \quad (4)$$

$$N_r = a_N\left(\frac{r}{R}\right)^2 + b_N \quad (5)$$

where r is the radial distance from the center of the column, R the column radius, u_r and N_r the linear flow velocity of the mobile phase and the number of theoretical plates at a radial position r, respectively, and a_u, b_u, a_N and b_N are numerical parameters. It is incorrect but most convenient to consider a radial distribution of the ''local column efficiency'' expressed as a number of theoretical plates. The plate number of the column is defined by reference to its length. The true local property is the apparent axial dispersion coefficient or the height equivalent to a theoretical plate. These three parameters are related through classical relationships ($H=2D_a/u=L/N$). However, the column efficiency is the best known parameter and, thus, the term ''local column efficiency'' is most convenient to use.

Since it was experimentally demonstrated that the relative variation of the flow velocity from near the wall of the column (u_w) to its center (u_c) is usually no more than a few percent [5–7,9,11–14], the ratio of u_w/u_c was varied from 1.0 to 1.1 with an

increment of 0.02. In all figures, except the first two, the lines are obtained at different values of N_w/N_c, by interpolation from the corresponding six calculated points. By contrast to the conditions selected in a previous paper, in which tailing was studied [19], it was assumed that the flow velocity near the wall was faster than that in the core region of the column. In order to eliminate trivial variations of the hold-up time with the extent of cross-section variation of the velocity, the flow-rate, hence the average mobile phase flow velocity (u_{av}), was kept constant, so that the first moment of the calculated peaks also remained constant and equal to unity (by normalization). The value of u_{av} is given by

$$u_{av} = \int_0^R 2\pi r \frac{u_r}{\pi R^2} dr \quad (6)$$

Combination of Eqs. (4) and (6) gives $u_{av} = (a_u/2) + b_u$. From Eq. (4), $u_c = b_u$, and $u_w = a_u + b_u$. Finally, the values of a_u and b_u were chosen so that u_{av} was equal to 1, as explained above. The calculation parameters, a_u and b_u, depend on the value of u_w/u_c. The values used were $a_u = 0$, $b_u = 1$ ($u_w/u_c = 1.00$); $a_u = 0.01980$, $b_u = 0.99010$ ($u_w/u_c = 1.02$); $a_u = 0.03922$, $b_u = 0.98039$ ($u_w/u_c = 1.04$); $a_u = 0.05826$, $b_u = 0.97087$ ($u_w/u_c = 1.06$); $a_u = 0.07692$, $b_u = 0.96154$ ($u_w/u_c = 1.08$); and $a_u = 0.09524$, $b_u = 0.95238$ ($u_w/u_c = 1.10$). Similarly, the ratio of N_w/N_c was varied from 0.2 to 1.0 with an increment of 0.2 in most cases because the HETP was shown to be several times larger near the wall than in the center of the column [5–7,9,11–14]. The values of a_N and b_N depend on both the ratio N_w/N_c and the value of N_c. When the calculation was made at $N_c = 1000$, the parameters were $a_N = -800$, $b_N = 1000$ ($N_w/N_c = 0.2$); $a_N = -600$, $b_N = 1000$ ($N_w/N_c = 0.4$); $a_N = -400$, $b_N = 1000$ ($N_w/N_c = 0.6$); $a_N = -200$, $b_N = 1000$ ($N_w/N_c = 0.8$); and $a_N = 0$, $b_N = 1000$ ($N_w/N_c = 1.0$).

3. Experimental

3.1. Apparatus

The measurements of elution peak profiles were made with a high-performance liquid chromatograph (LC-6A, Shimadzu, Kyoto, Japan) equipped with an ultraviolet detector and a Rheodyne (Cotati, CA, USA) sample injector (Model 7125). Small volumes (a few μl) of the sample solutions were used. The column temperature was kept constant by means of a temperature-controlled water bath.

3.2. Columns and reagents

We used five reversed-phase, 150×6 mm columns packed with chemically-bonded alkyl silica gels, i.e., C_1 (column 1), C_4 (column 2), C_8 (column 3), and C_{18} (columns 4 and 5), all from YMC (Kyoto, Japan). They were packed by the manufacturer, most probably using the slurry packing method. The carbon contents of the two C_{18}-silica gels were 6.6 and 17.1% (w/w). The average particle size was 45 μm. The advantage of using in this study packing materials with such coarse particles is the virtual elimination of the influence of extra-column volumes on the peak profile.

The mobile phase was methanol–water (70:30, v/v). Water was prepared by distillation of ion-exchanged water. Organic compounds, such as benzene, ethylbenzene, butylbenzene, hexylbenzene and naphthalene, were used as probe solutes. Uracil was used as the unretained tracer for the determination of the total porosity of the columns.

3.3. Procedure

The chromatographic peaks were usually recorded at 298 K and a mobile phase flow-rate of 2 ml/min. With naphthalene, the elution peaks were also recorded at 288 and 308 K and at 1 ml/min, in order to determine the influence of some variations of the experimental conditions on the results. No experiments using naphthalene were carried out for column 5 because this column seemed to have a small bed heterogeneity. Some parameters of the fronting peaks recorded, such as their width at 10 and 50% of the maximum peak height and their asymmetry factor at 10% of the peak height, were graphically measured. The asymmetry factor was defined as the ratio of the rear half-width of the elution peak (w_R) to the front half-width (w_F). In this study, 10 elution peaks were recorded for each column (except column 5), with different sample compounds, temperatures and mobile phase flow-rates. The experimental data were

compared with the calculation results to derive the required information on the correlation actually observed between N_w/N_c and u_w/u_c.

4. Results and discussion

We studied first the influence of the radial heterogeneity of the mobile phase flow velocity, second, the combined influence of the radial heterogeneity of both the velocity and the local dispersion coefficient on the fronting behavior of chromatographic peaks using a numerical method. Then, we analyze the characteristic features of the fronting peaks so calculated. Finally, new information regarding the column radial heterogeneity was derived from comparisons of experimental data previously reported with the characteristics of the fronting peaks resulting from our analyses.

4.1. Numerical calculations of elution peaks

In order to illustrate the origin of the asymmetry of elution peaks, profiles were calculated under the following five sets of conditions, (1) $u_w/u_c=1.0$, $N_w/N_c=1.0$; (2) $u_w/u_c=1.1$, $N_w/N_c=1.0$; (3) $u_w/u_c=1.0$, $N_w/N_c=0.2$; (4) $u_w/u_c=1.05$, $N_w/N_c=0.6$; and (5) $u_w/u_c=1.1$, $N_w/N_c=0.2$. Fig. 1 shows the chromatograms calculated in the first three cases. In the first case, the column was assumed to be radially homogeneous regarding both the flow velocity and the local dispersion. The elution peak has a Gaussian profile. In the second case, there is only a radial variation of the flow velocity while the local apparent dispersion coefficient is uniform across the column. The apical retention time is slightly below one, suggesting that the elution peak tails a little. The asymmetry factor is somewhat larger than unity. In the third case, the flow velocity is constant across the column but N_c is five-times larger than N_w. Compared with the Gaussian profile obtained in the first case, the two other profiles in Fig. 1 are wider. However, the asymmetry factor in the third case remains equal to one. Fig. 2 shows the peak profiles calculated under the first, fourth and fifth sets of conditions. In these last two cases, simultaneous radial distributions of the mobile phase flow velocity and the local apparent dispersion coefficient were

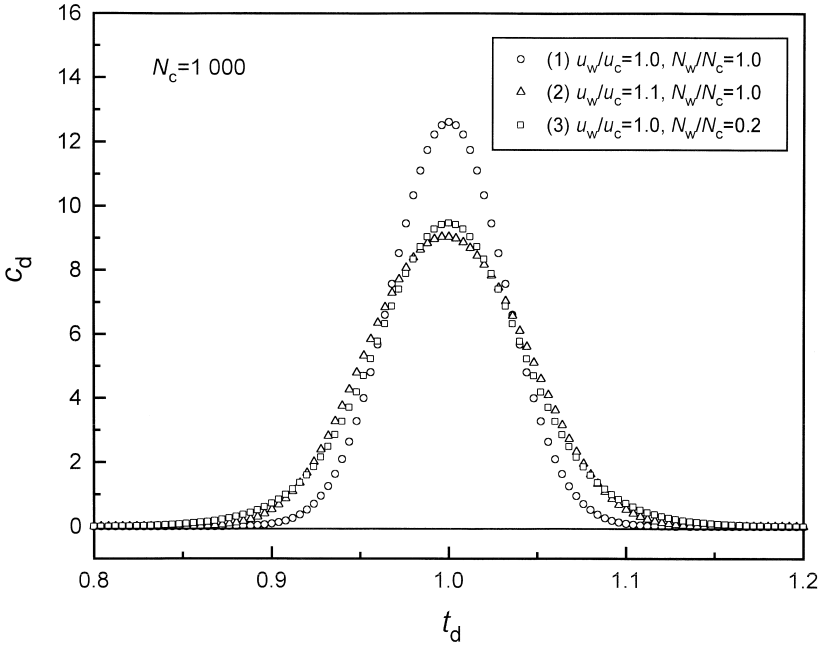

Fig. 1. Influence of the radial heterogeneity of the mobile phase flow velocity and the local apparent dispersion coefficient distributions on the peak profiles calculated.

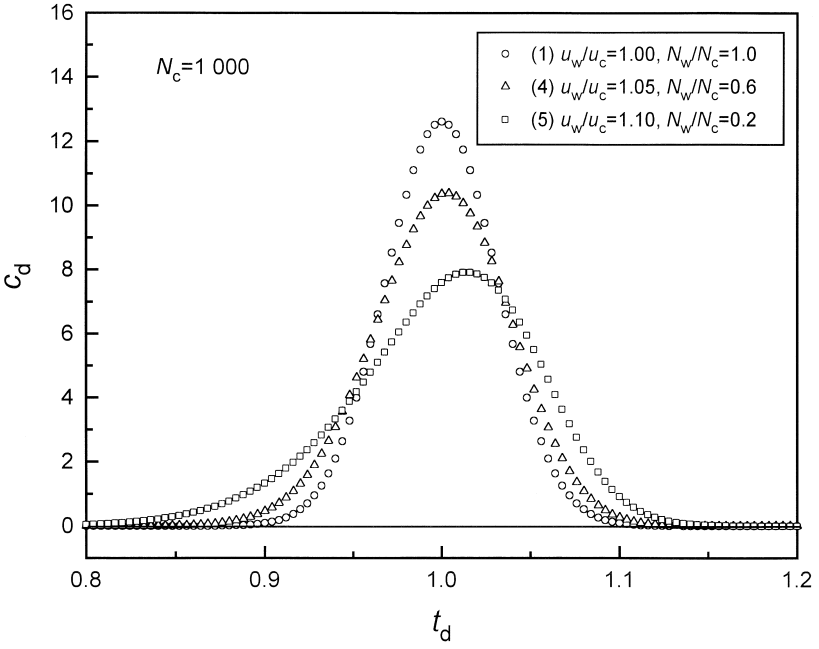

Fig. 2. Influence of the radial heterogeneity of the mobile phase flow velocity and the local apparent dispersion coefficient distributions on the peak profiles calculated.

assumed. The amplitude of the column radial heterogeneity increases in the order (1)<(4)<(5). Now the profiles calculated are unsymmetrical and the width and asymmetry of the peaks increase with increasing degree of column radial heterogeneity. The fifth peak exhibits an obvious fronting effect.

4.2. Influence of the single flow velocity distribution

Chromatographic peaks were calculated by considering only a flow velocity distribution, as described earlier (Eq. (4)), and assuming that the local apparent dispersion coefficient was constant across the column. Because of the radial velocity distribution, however, the apparent column efficiency, derived from the profile of the peak recorded by an on-line detector, is different from the constant local efficiency. Fig. 3 illustrates the relationship between the ratio of the apparent number of theoretical plates of the elution peak (N_M) and the value of N at the column center (N_c), on the one hand, and the amplitude of the radial variation of the flow velocity (u_w/u_c). The value of N_M was obtained from the following equation.

$$N_M = \frac{\mu_1^2}{\mu_2'} \tag{7}$$

where μ_1 is the first moment of the elution peak, which is always one in this study, as described above, and μ_2' is the second central moment, calculated by the following equation.

$$\mu_2' = \frac{\int C_d(t_d)(1-t_d)^2 dt_d}{\int C_d(t_d) dt_d} \tag{8}$$

where $C_d(t_d)$ is the dimensionless concentration at reduced time t_d. Fig. 3 shows that the influence of the flow velocity distribution is more severe on high efficiency columns than on low efficiency ones. Fig. 4 shows the influence of the amplitude of the flow velocity distribution on the asymmetry factor of the elution peak. The value of $(w_R/w_F)_{0.1}$, the asymmetry factor at 10% of the maximum peak

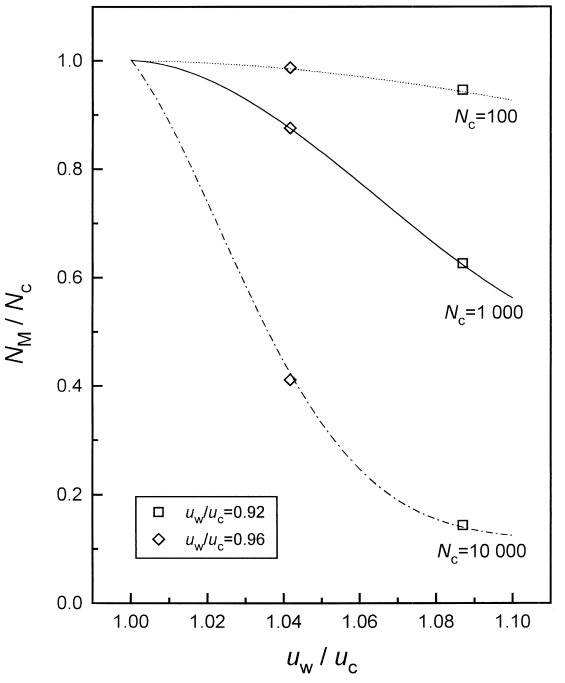

Fig. 3. Influence of the radial heterogeneity of the mobile phase flow velocity distribution on the apparent column efficiency. The radial distribution of the local apparent dispersion coefficient is assumed to be uniform. The symbols represent calculation results obtained previously [19] at $u_w/u_c=0.92$ (open square) and $u_w/u_c=0.96$ (open diamond). Because the direction of the presumed parabolic distribution of the flow velocity is opposite the one in this previous study [19], the values of 0.92 and 0.96 in the earlier work correspond approximately to 1.087 and 1.042, respectively.

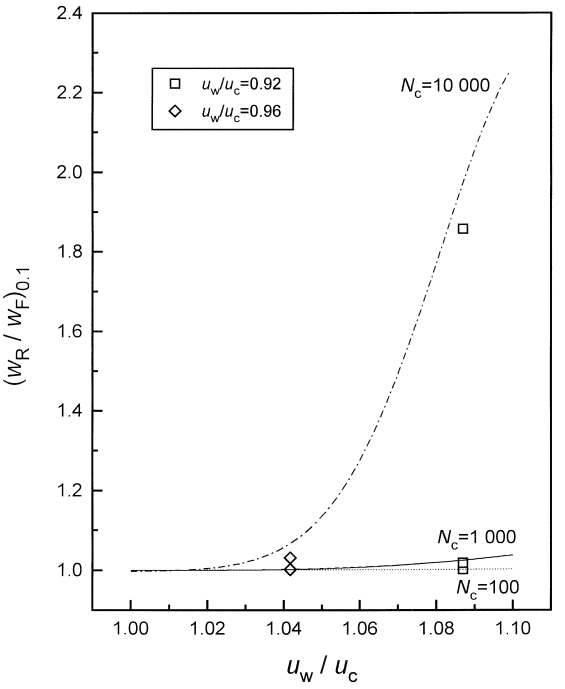

Fig. 4. Influence of the radial heterogeneity of the mobile phase flow velocity distribution on the asymmetry factor of the elution peak. The radial distribution of the local apparent dispersion coefficient is assumed to be uniform. The symbols (open square and open diamond) represent the calculation results in a previous paper [19] at $u_w/u_c=0.92$ (open square) and $u_w/u_c=0.96$ (open diamond), respectively. Because of the opposite directions of the presumed parabolic distribution of the flow velocity in the previous study [19] and in this paper, the values of 0.92 and 0.96 in the earlier work correspond approximately to 1.087 and 1.042, respectively.

height, increases with increasing degree of radial heterogeneity of the flow velocity. Practically, no tailing of the profile is predicted at $N_c=100$ and only a slight one at $N_c=1000$.

The calculation results discussed in a previous paper [19] at $u_w/u_c=0.92$ (open square) and $u_w/u_c=0.96$ (open diamond) are also shown in Figs. 3 and 4. However, the values of the maximum and the minimum of the flow velocity across the column in this study are the reverse of those used in the previous paper, i.e., here $u_w/u_c>1.0$ while in the previous work, $u_w/u_c<1.0$, so the values of 0.92 and 0.96 in this earlier work correspond approximately to 1.087 ($=1/0.92$) and 1.042 ($=1/0.96$), respectively. The agreement between the transposition of these earlier results and the new ones shown in Figs. 3 and 4 indicates that the calculation results exhibit the same trends, although there are minor deviations at $N_c=10\,000$. Finally, the results in Figs. 3 and 4 show that peak tailing is always observed under experimental conditions for which there is only a radial variation of the flow velocity, irrespective of the curvature of the parabolic distribution, whether the maximum velocity is at the column center or along its wall. This is the case of the peak profile calculated in the second case (open triangle) in Fig. 1. As indicated by Yun and Guiochon [21], the magnitude of the flow velocity distribution is more important than whether the maximum velocity is in the center or near the wall.

4.3. Combined influence of the radial distributions of the flow velocity and the local column efficiency

Now, the correlations between either N_M/N_c or $(w_R/w_F)_{0.1}$ and u_w/u_c depend on the extent of the radial variation of the local apparent dispersion coefficient. Similar to Figs. 3 and 4, Figs. 5 and 6 illustrate these two correlations for $N_c=1000$. In Figs. 5 and 6, the data points for $u_w/u_c=1.0$ correspond to the calculation results obtained at constant mobile phase flow velocity across the column but variable dispersion coefficient. The plots in Fig. 6 indicate that, in this case, $(w_R/w_F)_{0.1}$ is always one at $u_w/u_c=1.0$, irrespective of the value of N_w/N_c. In this case, only the peak width increases with increasing degree of radial variation of the local dispersion coefficient because the distribution of the flow velocity is uniform. No tailing nor fronting peak can be expected under this set of conditions. This is, for example, the case of the third peak illustrated in Fig. 1 (open squares). From these results, we conclude that symmetrical peaks are observed when the radial distribution of the flow velocity is flat. Un-

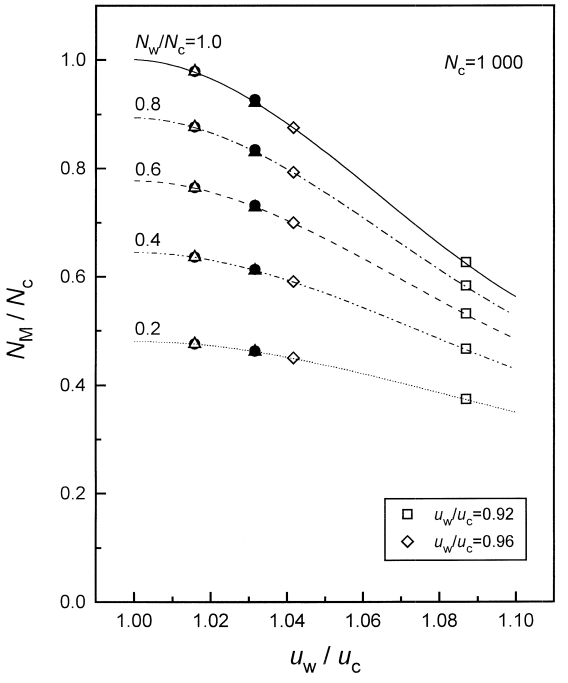

Fig. 5. Influence of the radial heterogeneity of the distributions of the mobile phase flow velocity and the local apparent dispersion coefficient on the apparent column efficiency. The local efficiency in the center region is 1000 theoretical plates. The circle and triangle symbols show calculation results at $N_c=100$, $u_w/u_c=1.05$ (open circle); $N_c=100$, $u_w/u_c=1.1$ (solid circle); $N_c=10\,000$, $u_w/u_c=1.005$ (open triangle); and $N_c=10\,000$, $u_w/u_c=1.01$ (solid triangle). The square and diamond symbols show calculation results for tailing peaks at $N_c=1000$, $u_w/u_c=0.92$ (open square) and $N_c=1000$, $u_w/u_c=0.96$ (open diamond). The open square and open diamond symbols show calculation results obtained previously [19] at $u_w/u_c=0.92$ (open square) and $u_w/u_c=0.96$ (open diamond). Because of the opposite directions of the presumed parabolic distribution of the flow velocity in the previous study [19] and in this paper, the values of 0.92 and 0.96 in the earlier work correspond approximately to 1.087 and 1.042, respectively.

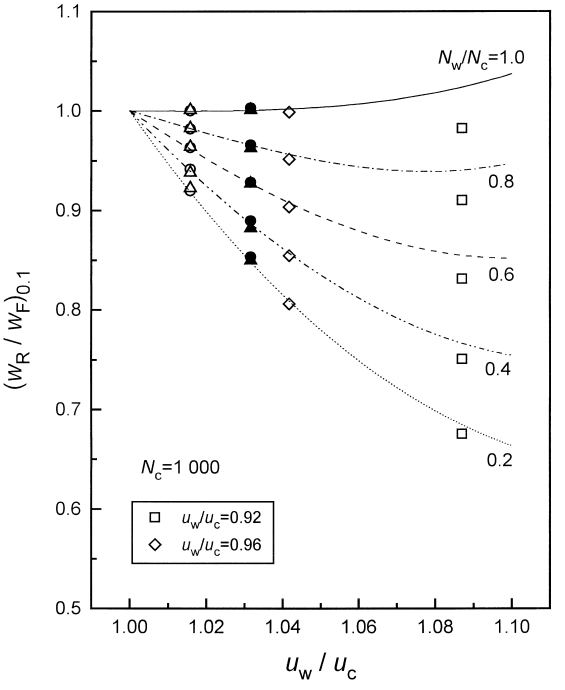

Fig. 6. Influence of the radial heterogeneity of the mobile phase flow velocity and the local apparent dispersion coefficient distributions on the asymmetry factor of the elution peak. The local efficiency in the center region is 1000 theoretical plates. The symbols are the same as in Fig. 5. The symbols (open square and open diamond) represent the calculation results obtained previously [19] at $u_w/u_c=0.92$ (open square) and $u_w/u_c=0.96$ (open diamond). Because of the opposite directions of the presumed parabolic distribution of the flow velocity in the previous study [19] and in this paper, the values of 0.92 and 0.96 in the earlier work correspond approximately to 1.087 and 1.042, respectively. In the cases when $u_w/u_c<1$ and $N_w/N_c<1$, tailing peaks were observed [19]. Peak fronting phenomena are analyzed in this study. The symbols (open square and open diamond) represent the reciprocal of the values of $(w_R/w_F)_{0.1}$ for the tailing peaks [19].

symmetrical peaks can be generated only when the velocity of the mobile phase is different in the center and the wall regions of the column.

By contrast, combinations of the influences of the radial distribution of the mobile phase flow velocity and of the local efficiency gives unsymmetrical peaks. Fig. 6 indicates that fronting peaks can be observed only when there are nonflat radial distributions of both the flow velocity and the local efficiency and if $u_w/u_c>1$. The degree of peak fronting increases with decreasing ratio N_w/N_c and with increasing ratio u_w/u_c. As an example, the value of $(w_R/w_F)_{0.1}$ approaches 0.66, a value corresponding to important peak fronting, for $u_w/u_c=1.1$ and $N_w/N_c=0.2$, a combination which is not unreasonable, as explained earlier. Fig. 6 also indicates that symmetrical or slightly tailing peaks are observed when the radial distribution of the column local efficiency is flat. The results in Fig. 5 indicate that peak spreading is enhanced when there is a strong fronting behavior. Compared to the Gaussian peak obtained with a column having flat distributions, the apparent value of μ_2' increases by a factor of nearly 3 under the conditions that $u_w/u_c=1.1$ and $N_w/N_c=0.2$. Finally, the results in Figs. 5 and 6 confirm that columns having a high efficiency are more sensitive to radial variations of the flow velocity than low efficiency columns.

In Figs. 5 and 6, the circle and triangle symbols indicate the results of similar calculations carried out at $N_c=100$ and 10 000, respectively. The solid symbols represent the results at $u_w/u_c=1.1$ and 1.01, respectively. Similarly, the open symbols represent those at $u_w/u_c=1.05$ and 1.005, respectively. The calculation values at $N_c=100$ and 10 000 are in agreement with each other, and can be plotted on the corresponding lines at $N_c=1000$, indicating that the range of u_w/u_c between 1.0 and 1.032 at $N_c=1000$ corresponds to that between 1.0 and 1.1 at $N_c=100$, and that between 1.0 and 1.01 at $N_c=10\,000$. In a previous paper [19], we have already reported similar correlations for elution peaks exhibiting a tailing profile. These correlations can be represented by the following equation.

$$\frac{\left(\frac{u_w}{u_c}\right)_i-1}{\left(\frac{u_w}{u_c}\right)_j-1}=\sqrt{\frac{N_j}{N_i}} \qquad (9)$$

where the subscripts i and j differentiate between two different columns. The values of N_i and N_j are the apparent numbers of theoretical plates of the overall elution peaks from the two radially heterogeneous columns i and j. Eq. (9) suggests that fronting peaks obtained with columns of different efficiencies exhibit similar shapes if their values of N_w/N_c are the same and that their fronting profiles can be correlated. It is probably possible to use this equation to make direct comparisons between the degrees of the radial variation of the flow velocity across the bed for columns having different efficiencies.

In practice, columns having a wide range of efficiencies, made by packing materials of quite different particle sizes and mass transfer performance, in columns of different lengths, are used in HPLC according to the nature and the difficulty of the separations to perform. The required values of the retention time and the peak width depend on the separation conditions. A useful comparison of the characteristics of fronting peaks obtained under this wide variety of experimental conditions can be made more simply by normalizing the peak width in addition to its first moment. Therefore, the results further discussed in this study were calculated at $N_c=1000$.

As they were in Figs. 3 and 4, the calculation results obtained in a previous paper [19] at $u_w/u_c=0.92$ (open square) and $u_w/u_c=0.96$ (open diamond) are also shown in Figs. 5 and 6 at $u_w/u_c=1.087$ and 1.042, respectively. In Fig. 5, the symbols are located on the corresponding lines, suggesting that the same overall efficiency is obtained, irrespective of the direction of the peak asymmetry. In a previous paper [19], we reported that tailing peaks were observed when $u_w/u_c<1.0$ and $N_w/N_c<1.0$. The reciprocal of the values of $(w_R/w_F)_{0.1}$ in the previous paper is plotted in Fig. 6 (open square and diamond). The symbols are close to the corresponding lines for the lower variation of the velocity but significantly below it for the larger one. The difference between the reciprocal of $(w_R/w_F)_{0.1}$ for tailing peaks in the previous paper and $(w_R/w_F)_{0.1}$ for fronting peaks in this study increases with increasing value of u_w/u_c. The results in Figs. 3 and 5 suggest that the influence of u_w/u_c, whether lower or higher than unity, on μ_2' can be correlated by defining the velocity ratio as lower than one. On the other hand, such a procedure

would not allow a correlation between u_w/u_c and the asymmetry factor, although the same trend is observed in Figs. 4 and 6.

4.3.1. Summary of the results derived from the numerical calculations

The experimental data concerning the radial heterogeneity of the flow velocity previously published [5–14] suggest that there are two types of distributions of u, i.e., $u_w/u_c<1$ and $u_w/u_c>1$. On the other hand, only one type of distribution was reported for N, i.e., $N_w/N_c<1$. A situation in which N_w is larger than N_c was never reported. From these observations, only six combinations of u_w/u_c and N_w/N_c need to be considered, (1) $u_w/u_c=1$, $N_w/N_c=1$; (2) $u_w/u_c=1$, $N_w/N_c<1$; (3) $u_w/u_c<1$, $N_w/N_c=1$; (4) $u_w/u_c>1$, $N_w/N_c=1$; (5) $u_w/u_c<1$, $N_w/N_c<1$; (6) $u_w/u_c>1$, $N_w/N_c<1$. In case (1), a Gaussian peak is observed because there is no radial distribution of either u or N across the column. In case (2), there is only a radial variation of N while u is uniform across the column. In such a case, the asymmetry factor of the elution peaks remains equal to unity. By contrast, in cases (3) and (4), N is constant across the column but u_w is smaller or larger than u_c, respectively. Under these conditions, only tailing peaks are observed, irrespective of the direction of the distribution of u. It seems reasonable that the peak tailing behavior is amplified with increasing degree of radial variation of u. A similar conclusion was reported by Yun and Guiochon [21]. Based on the ideal model of chromatography, they modeled the radial heterogeneity of a column and showed that the nature of the distribution of u was more important than whether the maximum velocity was located in the center or close to the wall. In previous papers [19,20], it was also shown that peak tailing was observed in case (5).

In this study, we analyzed peak profiles obtained under the conditions of case (6) and found that fronting peaks may be observed only in such a case. The experiments of Knox et al. [11] gave fronting peaks. His columns were dry-packed and their radial flow-rate and efficiency distributions correspond to case (6). Although fronting peaks were reported in linear chromatography using columns prepared by either dry- or slurry-packing methods, there may be no other interpretations for peak fronting behavior than the one presented here. We know of no alternate explanation of the origin of fronting behavior in linear chromatography. Because it is extremely complicated to analyze the influence of the column heterogeneity on the peak profile, we applied the numerical method discussed earlier to explain the peak asymmetry observed in linear chromatography. In the following, the influence of the radial heterogeneity of the column on fronting peak profiles is discussed.

4.4. Characteristics of fronting peaks

4.4.1. Retention time

In this study, the average flow velocity of the mobile phase was normalized so that the first moment, μ_1, of all the calculated peaks was equal to one. Fig. 7 shows a plot of the ratio of the apical retention time (t_R) to μ_1 as a function of u_w/u_c. The apical retention time is the apparent retention time while μ_1 is the true or thermodynamic retention time,

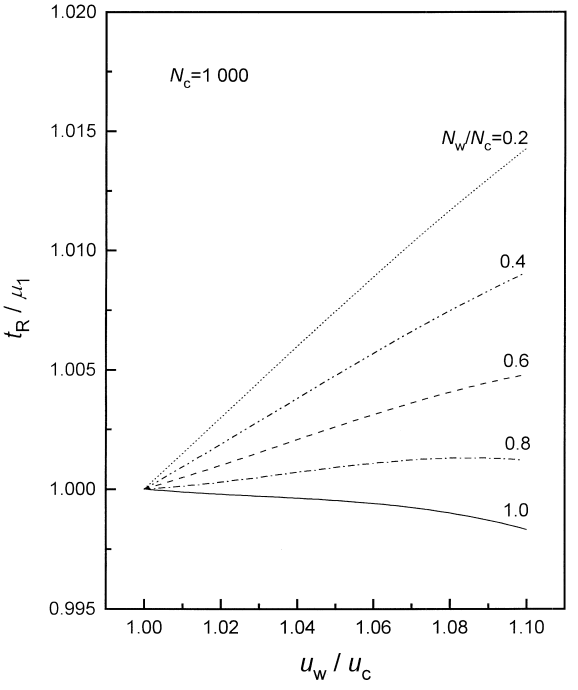

Fig. 7. Ratio of the apical retention time to the first moment of the elution peak as a function of the radial heterogeneity of the distributions of the mobile phase flow velocity and the local apparent dispersion coefficient.

which remains constant. The former time increases with increasing degree of peak fronting. It decreases when the elution peak exhibits a tailing profile at $N_w/N_c=1.0$ (cf. Fig. 6). The magnitude of the variation in t_R is not large, however. The relative variation is approximately 1.5% under such extreme conditions that $u_w/u_c=1.1$ and $N_w/N_c=0.2$. As illustrated in Figs. 5 and 6, the peaks observed under these conditions show considerable fronting, N_M being reduced to nearly one-third of N_c and $(w_R/w_F)_{0.1}$ being equal to approximately 0.66. The apical retention time is not a convenient indicator of the degree of bed heterogeneity.

4.4.2. Second central moment

Fig. 8 illustrates the influence of the radial distribution of the flow velocity on μ_2'. The ordinate is the ratio of μ_2', derived from Eq. (8), to the value of the second moment calculated from the column efficiency at the center of the column ($\mu_{2,c}'$). In Fig. 8, $\mu_{2,c}'=1\cdot10^{-3}$. The fronting behavior is accompanied with peak spreading. The second moment of the elution peak increases by a factor of about 2.9 over $\mu_{2,c}'$ under the extreme conditions selected, $u_w/u_c=1.1$ and $N_w/N_c=0.2$.

The apparent variance of the elution peak (σ^2) is conventionally derived from its peak width at half height ($w_{0.5}$) according to the following equation, which assumes a Gaussian profile.

$$\sigma_{0.5}^2=\frac{w_{0.5}^2}{5.54} \tag{10}$$

The column efficiency is conveniently represented by the number of theoretical plates ($N_{0.5}$) calculated by the following equation.

$$N_{0.5}=\frac{t_R^2}{\sigma_{0.5}^2} \tag{11}$$

Fig. 9 shows that, depending on the nature and the degree of heterogeneity of the column bed, the value

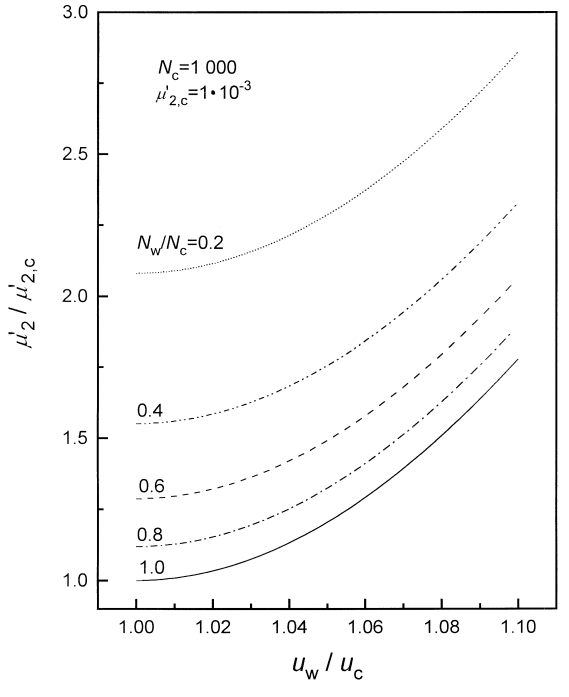

Fig. 8. Dependence of the second central moment of the elution peak on the radial heterogeneity of the mobile phase flow velocity and the local apparent dispersion coefficient distributions.

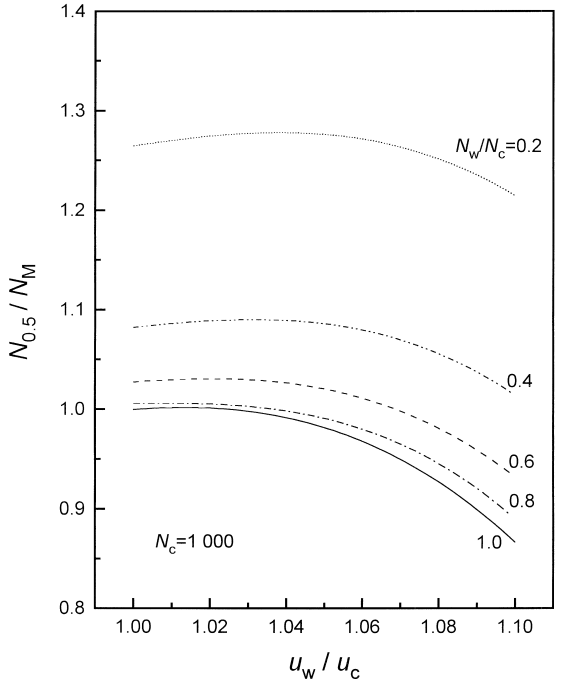

Fig. 9. Influence of the radial heterogeneity of the mobile phase flow velocity and the local apparent dispersion coefficient on the estimation of the apparent column efficiency. The column efficiency (number of theoretical plates) was calculated either from the first and the second central moments (N_M), or from the retention time and the peak variance derived from the width at 50% peak height ($N_{0.5}$).

of $N_{0.5}/N_M$ may be anywhere between 0.85 and 1.28. When the peak exhibits an unsymmetrical profile, there is no longer a correct definition of the column efficiency. Either expression given by Eqs. (7) or (11) can be larger than the other, depending on the particular case studied, although, in practice, larger values of $N_{0.5}$ compared to N_M are more frequently reported. Proper application of the contradictory results regarding $N_{0.5}/N_M$ could probably provide original information concerning the nature and degree of radial heterogeneity of the column.

4.4.3. Peak fronting behavior

Fig. 10 illustrates the influence of peak fronting on the variation of the peak width with the fractional height. The ratio $w_{0.5}/w_{0.1}$ is plotted against u_w/u_c for different values of the range of variation of the plate height. This ratio of the peak widths at 0.5- and 0.1-times the peak height is equal to 0.549 for a Gaussian peak. Fig. 11 shows the correlation between this ratio and u_w/u_c. The results in Fig. 11

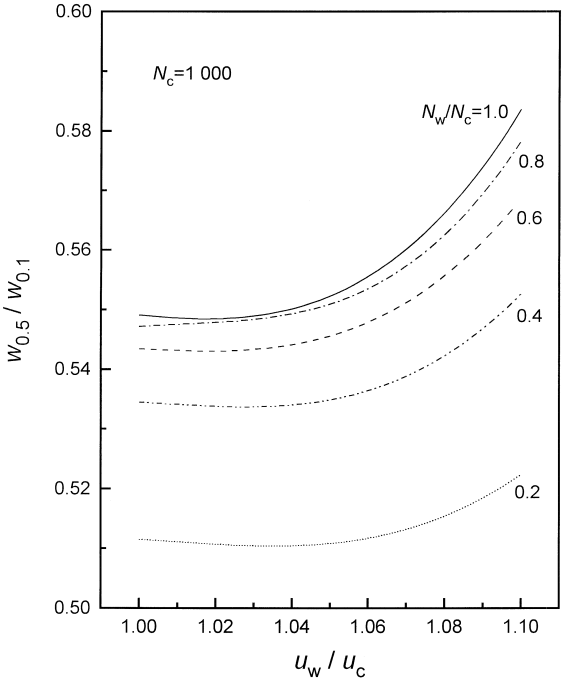

Fig. 10. Correlation of the peak widths at 10 and 50% of the peak height with the radial heterogeneity of the dispersions of the mobile phase flow velocity and the local apparent coefficient distributions.

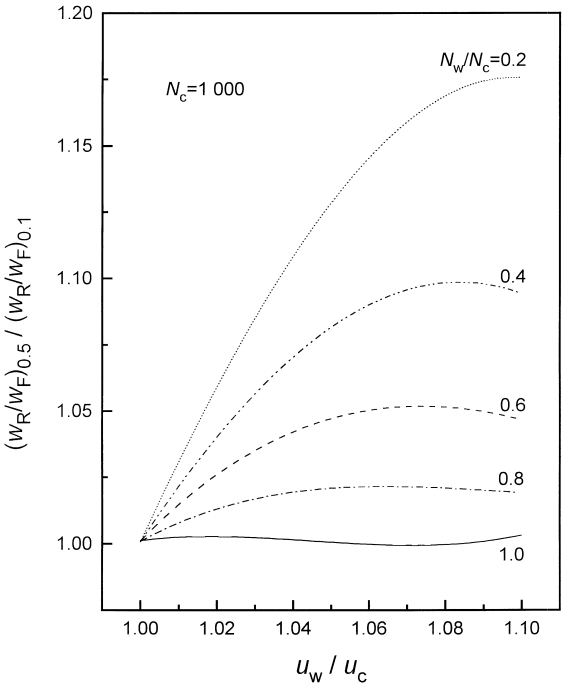

Fig. 11. Correlation between the peak asymmetry factors at 10 and 50% of the peak height and the radial heterogeneity of the distributions of the mobile phase flow velocity and the local apparent dispersion coefficient.

show that $(w_R/w_F)_{0.1}$ is always smaller than $(w_R/w_F)_{0.5}$ under all experimental conditions under which chromatographic peaks may exhibit fronting profiles.

4.5. Estimation of the radial heterogeneity of the flow velocity and the local efficiency

It is frequently observed that the variance calculated from Eq. (10) is smaller than μ_2' derived from Eq. (8), and that the value of $N_{0.5}$ afforded by Eq. (11) is an overestimate of the column efficiency. The peak profile is not Gaussian and widens faster than a Gaussian function when the relative height decreases. As described above, however, Fig. 9 suggests that $N_{0.5}/N_M$ smaller than unity are possible under certain combinations of radial distributions of the flow velocity and the local efficiency. It is expected that a comparison of experimental data and calculation results might provide new information about the column radial heterogeneity. In this study, peak fronting was characterized from the following

three viewpoints, (1) the ratio of the apical and thermodynamic retention times, (2) the width of the peak at different fractional heights, and (3) the peak asymmetry factors. The following parameters of the overall peaks, t_R/μ_1, $w_{0.5}/w_{0.1}$, $(w_R/w_F)_{0.5}$ and $(w_R/w_F)_{0.1}$, were calculated at $N_c=1000$ and analyzed. Supposing that there are two different efficiency columns A and B, of which N_w/N_c values are equal, and that the values of u_w/u_c in the both columns are correlated by Eq. (9), the elution peaks from the two columns might show similar shapes, that is, same characteristics of the peak profiles. The asymmetric factor at 10% peak height, $(w_R/w_F)_{0.1}$, would be equal as illustrated in Fig. 6. However, the peak widths are different for the elution peaks from the columns A and B. For example, when N_c is 10-times larger in the column A than B, w of the peak from the column B is larger than that from A by a factor of about 3.2 ($=\sqrt{10}$). Although the absolute values of w are different for the peaks, the ratios of w values might be same in a similar manner as $(w_R/w_F)_{0.1}$. On the other hand, the variation of t_R/μ_1 depends on N_c of the columns because the magnitude of the peak distortion is different between the columns A and B and because μ_1 is normalized in such a way that $\mu_1=1$. Except for t_R/μ_1, the ratios, i.e., $w_{0.5}/w_{0.1}$, $(w_R/w_F)_{0.5}$ and $(w_R/w_F)_{0.1}$, probably provide the same results, irrespective of the value of N_c, when fronting peaks given by columns of different efficiency have similar shapes.

4.5.1. Retention time of fronting peaks

Fig. 12 illustrates the correlation between t_R/μ_1 and $(w_R/w_F)_{0.1}$. The apical retention time increases with increasing degree of peak fronting. However, the magnitude of the variation of t_R is not large. The relative variation is approximately 1.5% even under the conditions that $(w_R/w_F)_{0.1}$ is about 0.66. However, the results in Fig. 12 indicate that the apical retention time depends only on the degree of the peak fronting. Almost same value of t_R/μ_1 can be obtained when $(w_R/w_F)_{0.1}$ values are same. The solid line in Fig. 12 is the correlation of the calculation results. Data points corresponding to different combinations of u_w/u_c and N_w/N_c can be found at the same place on the solid line. However, it cannot be expected that solid information about the degree of column radial heterogeneity will be obtained from

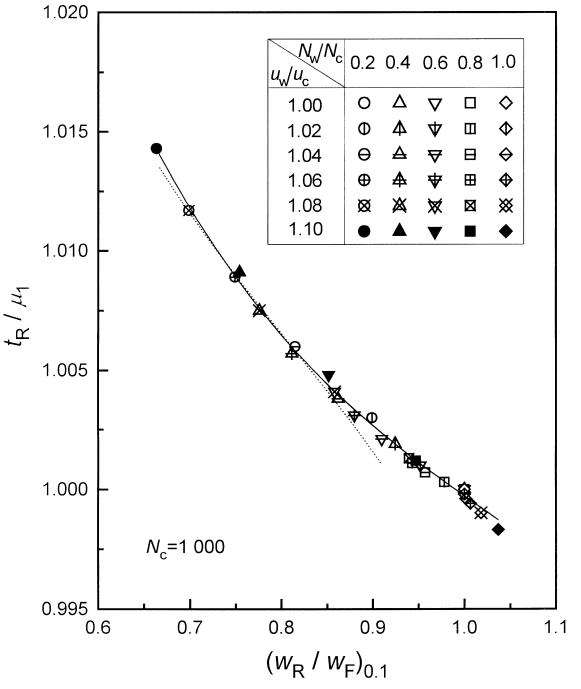

Fig. 12. Plot of the ratio of the apical retention time to the first moment of the elution peak versus the asymmetry factor at 10% of the maximum peak height. The local efficiency in the center region is 1000 theoretical plates. The symbols indicate results of calculations made under various conditions of N_w/N_c and u_w/u_c. The values of N_w/N_c are 0.2 (circle), 0.4 (up triangle), 0.6 (down triangle), 0.8 (square), and 1.0 (diamond). The values of u_w/u_c are 1.0 (open), 1.02 (with center vertical line), 1.04 (with center horizontal line), 1.06 (with center +), 1.08 (with center ×), and 1.1 (solid). The solid line is the correlation of the points calculated. The dotted line gives the correlation calculated by the equations derived from the exponentially modified Gaussian (EMG) function [24].

the comparison of the calculation results regarding t_R with experimental data. It would be difficult to determine the thermodynamic retention time with enough accuracy. Besides, Fig. 5 indicates that N_M is reduced to about one third of N_c under the conditions that $(w_R/w_F)_{0.1}$ is 0.66, suggesting that the peak width is more sensitive to radial variations of the column properties than t_R.

Attempts were made in the past at representing the tailing profiles of chromatographic peaks by using different functions. Foley and Dorsey analyzed numerically the characteristics of tailing peaks using the exponentially modified Gaussian (EMG) function and derived some empirical equations for tailing

peaks [24]. Some graphically measurable parameters of tailing peaks were correlated with the parameters of the EMG function. Two parameters measured at 10% of the maximum peak height were studied, $w_{0.1}$ and $(w_R/w_F)_{0.1}$, and the following equations were proposed [24]

$$\mu_2' = w_{0.1}^2/\left[1.764(w_R/w_F)_{0.1}^2 - 11.15(w_R/w_F)_{0.1} + 28\right] \quad (12)$$

$$\sigma_G = w_{0.1}/\left[3.27(w_R/w_F)_{0.1} + 1.2\right] \quad (13)$$

$$t_G = t_R - \sigma_G\left[-0.193(w_R/w_F)_{0.1}^2 + 1.162(w_R/w_F)_{0.1} - 0.545\right] \quad (14)$$

where t_G and σ_G are the retention time and the standard deviation of the parent Gaussian peak from which the skewed EMG peak is derived, respectively. The other equations using the two parameters at 50% peak height, i.e., $w_{0.5}$ and $(w_R/w_F)_{0.5}$, are also reported.

$$\mu_2' = w_{0.5}^2/\left[-8.28(w_R/w_F)_{0.5}^3 + 41.8(w_R/w_F)_{0.5}^2 - 72.3\,(w_R/w_F)_{0.5} + 44.6\right] \quad (15)$$

$$\sigma_G = w_{0.5}/2.5(w_R/w_F)_{0.5} \quad (16)$$

$$t_G = t_R - \sigma_G\left[-1.46(w_R/w_F)_{0.5}^2 + 5(w_R/w_F)_{0.5} - 3.14\right] \quad (17)$$

Although Foley and Dorsey derived similar equations using the same two parameters but measured at 30% peak height, they recommended the use of Eqs. (12)–(14). According to the EMG function, μ_1 and μ_2' are given by the following equations [25]

$$\mu_1 = t_G + \tau \quad (18)$$

$$\mu_2' = \sigma_G^2 + \tau^2 \quad (19)$$

where τ is the time constant of the exponential of the EMG. Combination of Eqs. (12)–(14), (18) and (19) gives the following equation for tailing peaks.

$$(\mu_1 - t_R)/t_R = (\sigma_G/t_G)\{[\{f_2(w_R/w_F)_{0.1}\}^2/f_1(w_R/w_F)_{0.1} - 1]^{1/2} - f_3(w_R/w_F)_{0.1}\}/\left[1 + (\sigma_G/t_G)f_3(w_R/w_F)_{0.1}\right] \quad (20)$$

where $f_1(w_R/w_F)_{0.1}$, $f_2(w_R/w_F)_{0.1}$ and $f_3(w_R/w_F)_{0.1}$ are derived from Eqs. (12)–(14) and are written as follows.

$$f_1(w_R/w_F)_{0.1} = 1.764(w_R/w_F)_{0.1}^2 - 11.15(w_R/w_F)_{0.1} + 28 \quad (21)$$

$$f_2(w_R/w_F)_{0.1} = 3.27(w_R/w_F)_{0.1} + 1.2 \quad (22)$$

$$f_3(w_R/w_F)_{0.1} = -0.193(w_R/w_F)_{0.1}^2 + 1.162(w_R/w_F)_{0.1} - 0.545 \quad (23)$$

The dotted line in Fig. 12 illustrates the correlation between t_R/μ_1 and $(w_R/w_F)_{0.1}$ calculated by Eq. (20). In this figure, the reciprocals of both t_R/μ_1 and $(w_R/w_F)_{0.1}$ are plotted, to compensate for the difference in the direction of the asymmetry of a fronting peak compared to that of a tailing peak. For example, t_R/μ_1 for the tailing peak at $N_c = 1000$ and $(w_R/w_F)_{0.1} = 1.25$ can be calculated as 0.99334 using Eq. (20). So, the reverse value of 1.0067 is plotted as t_R/μ_1 for the fronting peak at $(w_R/w_F)_{0.1} = 0.8$. Although a similar trend is observed between the dotted and the solid line on the whole, the dotted line exhibits a different profile at high values of $(w_R/w_F)_{0.1}$. Eq. (20) is probably effective for tailing peaks in the range of $(w_R/w_F)_{0.1}$ larger than 1.09 because Eq. (13) is valid at $(w_R/w_F)_{0.1} > 1.09$. Eqs. (12)–(14) derived from the EMG function cannot be used for the analysis of the variation of the retention time due to peak fronting when $(w_R/w_F)_{0.1}$ is between 0.9 and 1.0.

4.5.2. Width of fronting peaks

The comparison of the results in Figs. 7 and 8 shows that μ_2' is more sensitive to the peak distortion than μ_1. Furthermore, the peak profiles in Fig. 2 suggest that fronting peaks are wider and shorter than symmetrical peaks. The ratio of the peak widths at different fractional heights may represent one of the characteristic features of fronting peaks. The correlation between $w_{0.5}/w_{0.1}$ and $(w_R/w_F)_{0.1}$ is

illustrated in Fig. 13. The calculated data points are widely scattered. The ratio of $w_{0.5}/w_{0.1}$ is equal to 0.549 for a Gaussian profile. As illustrated earlier, the value of $w_{0.5}/w_{0.1}$ depends on the nature and degree of radial heterogeneity of the column. Different combinations of values of u_w/u_c and N_w/N_c give different values of $w_{0.5}/w_{0.1}$ even at constant value of $(w_R/w_F)_{0.1}$. The results in Fig. 13 suggest that the comparison of the calculation results with experimental data could provide valuable information on the column radial heterogeneity.

Some experimental data measured on fronting peaks obtained with the five columns described earlier are compared with the calculation results in Fig. 14. It was already suggested, in connection with the theoretical results in Fig. 10, that values of $w_{0.5}/w_{0.1}$ larger than 0.549 may be observed with fronting peaks, under certain experimental conditions. The plot shown in Fig. 14 confirms this.

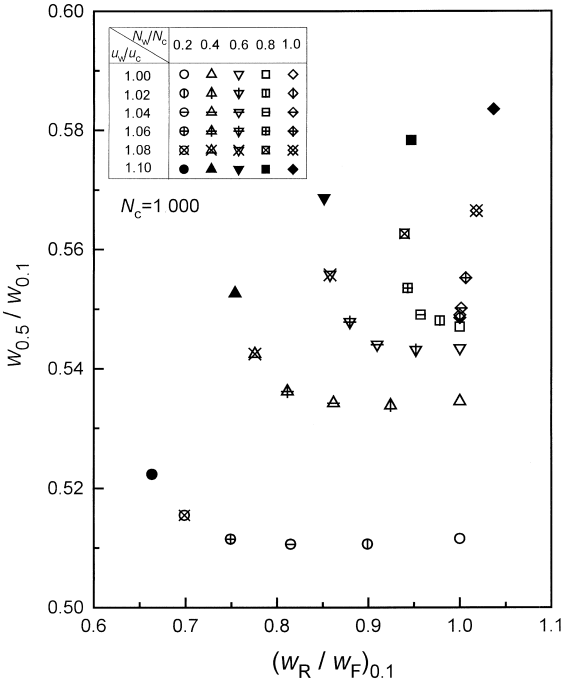

Fig. 13. Correlation of the ratio of the peak widths at 10 and 50% of the maximum peak height with the asymmetry factor at 10% peak height. The local efficiency in the center region is 1000 theoretical plates. The symbols indicate the results of calculations made under various conditions of N_w/N_c and u_w/u_c which are same as in Fig. 12.

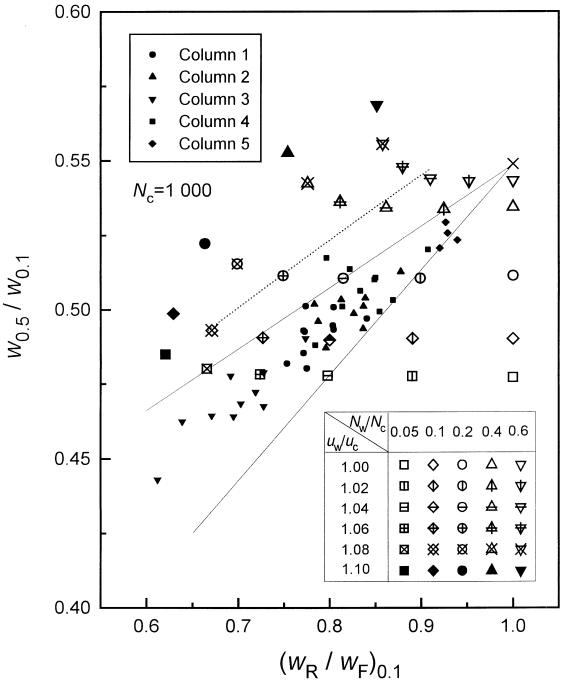

Fig. 14. Correlation of the ratio of the peak widths at 10 and 50% of the maximum peak height with the asymmetry factor at 10% peak height. The local efficiency in the center region is 1000 theoretical plates. The symbols indicate the results of calculations made under various conditions of N_w/N_c and u_w/u_c. The values of N_w/N_c are 0.05 (square), 0.1 (diamond), 0.2 (circle), 0.4 (up triangle), 0.6 (down triangle). The values of u_w/u_c are 1.0 (open), 1.02 (with center vertical line), 1.04 (with center horizontal line), 1.06 (with center +), 1.08 (with center ×), and 1.1 (solid). The experimental data are represented by small solid symbols for column 1 (solid circle), column 2 (solid up triangle), column 3 (solid down triangle), column 4 (solid square), and column 5 (solid diamond). The two solid lines indicate the range within which experimental data could be recorded in this study. The dotted line represents the correlation calculated by the equations derived from the EMG function.

However, the experimental data are all located in a narrowly limited region, between the two solid lines in Fig. 14. The experimental values of $w_{0.5}/w_{0.1}$ decrease from the point corresponding to the Gaussian curve with decreasing $(w_R/w_F)_{0.1}$. The results in Fig. 14 probably indicate the range of values of u_w/u_c and N_w/N_c which are observed in practice.

The dotted line in Fig. 14 illustrates the correlation between $w_{0.5}/w_{0.1}$ and $(w_R/w_F)_{0.1}$ derived from the equations of Foley and Dorsey [24]. The following equation is derived form Eqs. (13) and (16).

$$w_{0.5}/w_{0.1} = 2.5(w_R/w_F)_{0.5}/[3.27(w_R/w_F)_{0.1} + 1.2] \quad (24)$$

The correlation between $(w_R/w_F)_{0.1}$ and $(w_R/w_F)_{0.5}$ can be calculated by combining Eqs. (14) and (17). As done already for Fig. 12, the values of $w_{0.5}/w_{0.1}$ calculated with Eq. (24) for tailing peaks were converted into values for fronting peaks. For example, $w_{0.5}/w_{0.1}$ is calculated as 0.523 for a tailing peak with $(w_R/w_F)_{0.1} = 1.25$, the value of $(w_R/w_F)_{0.5}$ being calculated as 1.11, using Eqs. (14) and (17). The value of $w_{0.5}/w_{0.1}$ is also 0.523 for the fronting peak, with an asymmetry factor which is now 0.8. The dotted line shows a correlation which does not match the experimental data. These data suggest rather that there are various combinations of u_w/u_c and N_w/N_c leading to the same data points, although, in practice, the ranges of their variations are limited. The dotted line expresses the peak fronting characteristics only under extreme conditions, rarely matched in actual practice.

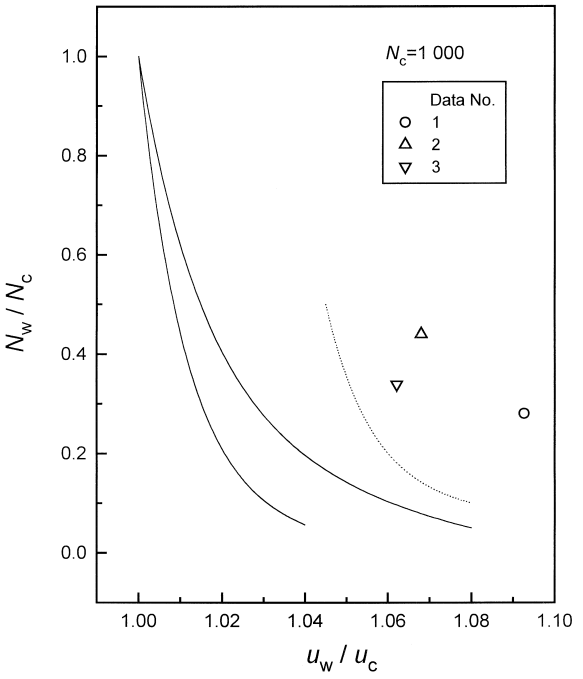

Fig. 15. Correlation between the radial heterogeneities of the distributions of the mobile phase flow velocity and the local apparent dispersion coefficient. The local efficiency in the center region is 1000 theoretical plates. The three plots represent the experimental results obtained in independent studies [11,12]. Data numbers refer to Table 1. The two solid lines indicate the range within which experimental data could be recorded in this study. The dotted line represents the correlation calculated by the equations derived from the EMG function.

4.5.3. Radial distribution of u_w/u_c and N_w/N_c

Fig. 15 illustrates the correlation between u_w/u_c and N_w/N_c. The two solid lines in Fig. 15 were calculated from those in Fig. 14. The amplitude of the distribution of the local efficiency increases with increasing amplitude of the flow velocity distribution. The results in Fig. 15 suggest that it is hardly possible to observe experimental data in the region corresponding to a radial heterogeneity of the column which affects the distribution of only either the flow velocity or the local efficiency. Obviously, both should coexist because they originate both from an heterogeneously packed bed [23]. We have already confirmed a similar situation for tailing peaks [20].

There are few experimental data collected under conditions in which the radial distributions of the flow velocity and the local efficiency could lead to fronting peaks. Knox et al. [11] measured these distributions on a glass column, dry-packed with glass beads (Table 1), using a dual-electrode polarographic detector. One electrode was fixed at the center of the outlet frit of the column, the other was moved across it. The concentration–time profiles at the column center and near the wall were measured by introducing a sample solution across the entire column section. The sample solution was prepared by dissolving *p*-nitrophenol in oxygen-free water containing 0.1 *M* KCl. Eon [12] made nearly the same measurements using almost the same experimental setup as Knox et al. He used two different columns, both dry-packed with glass beads (Table 1). One was a conventional stainless steel column, the other was made of PTFE and was radially compressed during the experiments. The three symbols in Fig. 15 represent these experimental data [11,12].

In this study, the values of u_w/u_c, determined experimentally at the original values of N_c in each experiment were converted to those at $N_c = 1000$ by applying Eq. (9). The results are reported in Table 1. Although these data points are not located between the two solid lines in Fig. 15, they do suggest that

Table 1
Experimental data on the radial heterogeneity of the mobile phase flow velocity and the column local apparent dispersion coefficient

Column			Efficiency			Radial heterogeneity			Data No.	Ref.
Packing materials	d_p[a] (μm)	Size (mm)	h_c[b]	h_w[c]	N_c[d]	N_w/N_c[e]	$u_w/u_c(N_c)$[f]	$u_w/u_c(1000)$[g]		
Glass beads	64	775×11.7	1.7	6.1	7100	0.28	1.03	1.09	1	[11]
Glass beads	76	600×17.3	1.6	3.5	5100	0.44	1.03	1.07	2	[12]
Glass beads	76	600×15.8	1.7	4.9	4800	0.34	1.03	1.06	3	[12]

[a] Particle diameter.
[b] Reduced HETP at the center of the column.
[c] Reduced HETP near the wall of the column.
[d] Number of theoretical plates at the center of the column.
[e] Ratio of the local apparent dispersion coefficient at the center to that near the wall of the column.
[f] Ratio of the flow velocity near the wall to that at the center of the column at each experimental condition.
[g] Conversion ratio of the flow velocity near the wall to that at the center of the column under the assumption that N_c is equal to 1000.

nonflat radial distributions of the mobile phase flow velocity and of the local efficiency coexist in the column. The discrepancy may result from experimental errors in the determination of u_w/u_c. The experimental data were originally measured at N_c = 5000–7000. In such cases, a relatively large error takes place when the values of u_w/u_c are converted using Eq. (9). It is necessary to acquire more experimental data on the nature and extent of the radial heterogeneity in columns which provide fronting peaks in order to validate the correlations shown in Fig. 15. However, the results in Figs. 14 and 15 already suggest that the degree of radial heterogeneity of the flow velocity and the local efficiency may be estimated by analyzing the information available in the overall peak profile, namely the band widths at different fractional peak height and the asymmetry factor. The dotted line in Fig. 15 shows the correlation between N_w/N_c and u_w/u_c calculated from that in Fig. 14. The dotted lines in Figs. 14 and 15 suggest that the EMG function cannot provide a comprehensive representation of the various types of fronting profiles in chromatography.

4.5.4. Asymmetry of fronting peak

Likewise the peak width at different fractional heights, the asymmetry factor at different peak heights is related with the characteristics of fronting peaks. The correlation between $(w_R/w_F)_{0.5}$ and $(w_R/w_F)_{0.1}$ is illustrated in Fig. 16. By contrast with the results in Figs. 13 and 14, the plots are not widely scattered. So, we cannot expect to obtain the information we need on the column radial heterogeneity from a comparison between calculation results and experimental data on peak asymmetry. The results in Fig. 16 indicate that $(w_R/w_F)_{0.1}$ is smaller than $(w_R/w_F)_{0.5}$ when chromatographic

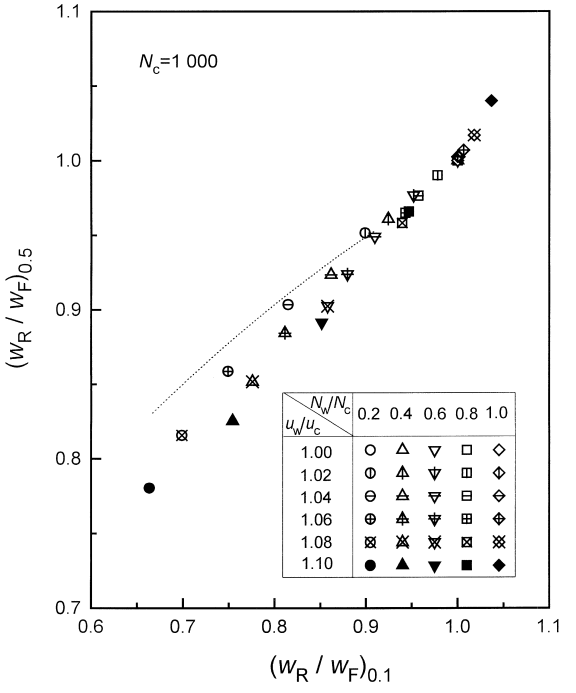

Fig. 16. Correlation between the asymmetry factors at 10 and 50% of the maximum peak height. The local efficiency in the center region is 1000 theoretical plates. The symbols indicate the results of calculations made under various conditions of N_w/N_c and u_w/u_c which are the same as in Fig. 12. The dotted line represents the correlation calculated by the equations derived from the EMG function.

peaks exhibit the fronting profiles. The correlation based on the EMG function (dotted line) shows a different tendency from that of the calculation plots in this study.

5. Conclusion

The origin of fronting behavior in linear chromatography is most probably in a suitable combination of the radial distributions of the flow velocity ($u_w/u_c>1$) and of the local efficiency ($N_w/N_c<1$). Peak tailing only arises when there is a radial distribution of the flow velocity (with either $u_w/u_c>1$ or $u_w/u_c<1$) and a flat distribution of the column efficiency. The asymmetry factor is constantly equal to one if there is only a radial distribution of the local efficiency. It becomes lower than one if the conditions above are satisfied and decreases with increasing amplitude of the local efficiency distribution. The influence of the column radial heterogeneity is more important for high efficiency columns than for low efficiency ones. Peak fronting behavior resulting from the radial heterogeneity of columns having different efficiency can be correlated by Eq. (9). The comparison of experimental data with the results of numerical calculations provided new information regarding the effects of column radial heterogeneity. An estimation of the degree of column radial heterogeneity is probably possible by analyzing the widths and the asymmetry factor of the fronting peaks. It was also found that the EMG function represented the fronting peak profiles at extremely limited conditions.

It is not intuitive that a parabolic velocity distribution should result in a tailing peak if the velocity is maximum in the column center and a fronting peak if it is minimum. A physical explanation is in order. This is because the velocity varies slowly in the center region (around its extremum) but rapidly close to the column wall. A large fraction of the solute elutes together at velocities close to the center velocity while a very small amount of solute only moves at the velocity corresponding to the mobile phase velocity close to the column wall. This fundamental dissymmetry explains the peak asymmetry.

6. Symbols

a_N, Coefficient in Eq. (5)
a_u, Coefficient in Eq. (4)
A_p, Area of the injected pulse
b_N, Coefficient in Eq. (5)
b_u, Coefficient in Eq. (4)
C, Actual solute concentration
C_d, Dimensionless concentration
$f_1(w_R/w_F)_{0.1}$, Defined in Eq. (21)
$f_2(w_R/w_F)_{0.1}$, Defined in Eq. (22)
$f_3(w_R/w_F)_{0.1}$, Defined in Eq. (23)
k'_0, Retention factor at infinite dilution
L, Column length
n, Amount of the solute injected
N, Number of theoretical plates
N_M, Defined in Eq. (7)
N_r, Number of theoretical plates at a radial position r
$N_{0.5}$, Defined in Eq. (11)
r, Radial distance from the center of the column
R, Column radius
S, Column cross-sectional area
t, Time
t_d, Dimensionless time
t_R, Retention time
u, Interstitial velocity of the mobile phase
u_{av}, Average mobile phase flow velocity
u_r, Linear velocity at a radial position r
w, Peak width
w_F, Front half-width of the elution peak
w_R, Rear half-width of the elution peak
w_R/w_F, Asymmetry factor

6.1. Greek

ϵ, Total porosity of the column
μ_1, First moment
μ'_2, Second central moment
σ, Standard deviation
σ_d, Dimensionless standard deviation
τ, Time constant of the exponential modifier

6.2. Subscripts

c, At the center of the column
G, Parent Gaussian constituent
i, ith column
j, jth column
w, Near the wall of the column

0.1, At 10% of maximum peak height
0.5, At 50% of maximum peak height

Acknowledgements

This work was supported in part by Grant CHE-97-01680 of the National Science Foundation and by the cooperative agreement between the University of Tennessee and the Oak Ridge National Laboratory. We acknowledge the support of Maureen S. Smith in solving our computational problems.

References

[1] G. Guiochon, S. Golshan-Shirazi, A.M. Katti, Fundamentals of Preparative and Nonlinear Chromatography, Academic Press, Boston, MA, 1994.
[2] J.C. Giddings, Dynamics of Chromatography, Marcel Dekker, New York, 1965.
[3] T. Fornstedt, G. Zhong, G. Guiochon, J. Chromatogr. A 741 (1996) 1.
[4] T. Fornstedt, G. Zhong, G. Guiochon, J. Chromatogr. A 742 (1996) 55.
[5] T. Farkas, M.J. Sepaniak, G. Guiochon, J. Chromatogr. A 740 (1996) 169.
[6] T. Farkas, M.J. Sepaniak, G. Guiochon, AIChE J. 43 (1997) 1964.
[7] T. Farkas, G. Guiochon, Anal. Chem. 69 (1997) 4592.
[8] T. Yun, G. Guiochon, J. Chromatogr. A 760 (1997) 17.
[9] T. Farkas, J.Q. Chambers, G. Guiochon, J. Chromatogr. A 679 (1994) 231.
[10] D.S. Horne, J.H. Knox, L. McLaren, Sep. Sci. 1 (1966) 531.
[11] J.H. Knox, G.L. Laird, P.A. Raven, J. Chromatogr. 122 (1976) 129.
[12] C.H. Eon, J. Chromatogr. 149 (1978) 29.
[13] J.E. Baur, E.W. Kristensen, R.M. Wightman, Anal. Chem. 60 (1988) 2334.
[14] J.E. Baur, R.M. Wightman, J. Chromatogr. 482 (1989) 65.
[15] E. Bayer, E. Baumeister, U. Tallarek, K. Albert, G. Guiochon, J. Chromatogr. A 704 (1995) 37.
[16] U. Tallarek, E. Baumeister, K. Albert, E. Bayer, G. Guiochon, J. Chromatogr. A 696 (1995) 1.
[17] U. Tallarek, K. Albert, E. Bayer, G. Guiochon, AIChE J. 42 (1996) 3041.
[18] U. Tallarek, E. Bayer, G. Guiochon, J. Am. Chem. Soc. 120 (1998) 1494.
[19] K. Miyabe, G. Guiochon, J. Chromatogr. A 830 (1999) 263.
[20] K. Miyabe, G. Guiochon, J. Chromatogr. A 830 (1999) 29.
[21] T. Yun, G. Guiochon, J. Chromatogr. A 672 (1994) 1.
[22] T. Yun, G. Guiochon, J. Chromatogr. A 734 (1996) 97.
[23] G. Guiochon, T. Farkas, H. Guan-Sajonz, J.-H. Koh, M. Sarker, B.J. Stanley, T. Yun, J. Chromatogr. A 762 (1997) 83.
[24] J.P. Foley, J.G. Dorsey, Anal. Chem. 55 (1983) 730.
[25] E. Grushka, Anal. Chem. 44 (1972) 1733.